The influence of paper surface energy on multicolor offset print mottling

JURAJ GIGAC, MIROSLAVA KASAJOVÁ, AND MONIKA STANKOVSKÁ

ABSTRACT: An evaluation of a series of commercial uncoated, semimatte, and glossy coated woodfree papers for the multicolor sheet-fed offset press is presented. This study is aimed at better understanding of mutual influences of surface free energy, paper surface roughness, and fountain solution on print mottling occurring in full-scale printing conditions. Each paper has unique structure in terms of surface roughness, porosity, and surface energy that are the result of manufacturing technology. At the point of contact of liquid with paper, the surface dynamic process of liquid absorption by paper occurs, involving phenomena such as wetting, penetration, diffusion, and swelling. Mottling of colored surface printed by cyan, magenta, yellow, and black inks copied the surface roughness of coated paper. Mottling in the second, third, and fourth printing units showed deviation from mottling in the first printing unit, depending on surface free energy of paper and on the frequency of paper-surface wetting by fountain solution before and after printing.

Application: Paper manufacturers, converters, and printers can use the results to optimize coating, surface calendering, and printing press conditions.

The uneven appearance of the image observed on prints can be caused by paper and ink quality or by the printing process. Mottling is seen as uneven coverage of paper surface by ink or as local differences of print density or print gloss caused by a wrong combination of offset blanket properties, fountain solution, ink and paper [1].

Several categories of mottling have been described [2–5]. Single ink mottling is caused by uneven absorbency of paper and by ink flocculation. Back trap mottling (BTM) is most frequently seen in the ink printed in the first or second printing unit of a multicolor offset printing. The cause lies in a partially variable absorption of ink into the paper. The partially variable immobilization of the ink leads to a variable splitting of the ink on the following blankets. Shaw and Eby [4] developed a methodology for analyzing both the surface and cross-sectional distribution of coating components using X-ray microanalyses and image analysis technology. Results of analyses were used to explain reasons of BTM. Some of their findings pertained to nonuniform concentrations of binder at the surface. Areas within a print that exhibited undesirable low ink density were found to have higher latex concentration. These areas also had a higher mean coating thickness. The higher mean coating thickness was related to lower mean raw-stock roughness. The lack of uniformity of calcium carbonate concentration on the surface of a finished paper was newly identified as a mechanism that may cause BTM. In addition the authors quote that, by supercalendering, areas of differential surface gloss and differential porosity are formed. They also predicate correlation between areas of high gloss and areas of low ink density. According to Plowman-Sandreuter [5] the most important characteristic of BTM is that it requires a combination of conditions to occur, and these are the four properties that are measured in the following studies: (a) multiple printing unity, (b) fast-setting ink, (c) a fast-setting paper, and (d) nonuniform paper absorption. Another cause of mottling can be imperfect or uneven absorption of fountain solution into paper before applying ink—water interference mottling (WIM). The unique characteristics of this type of print mottle are (a) that it requires only a single printing unit to occur and (b) any ink formulation can have WIM [5]. Although WIM occurs throughout the job, it is most offensive in screen areas and halftone pictures. WIM dots have ragged edges and WIM solids are broken and discontinuous, leaving a mottled, washed-out look to the print. Measured densities are typically low. Fountain solution applied in the next printing units causes a positive effect—equalizing of ink on paper surface printed in the previous printing unit [2,3].

Other studies of coated offset papers properties also showed that print quality (print mottling and ink setting rate) is significantly affected by formation [6], surface roughness [7,8], porosity, and wettability of paper [6,9,10]. However, fountain solution applied in a previous printing unit causes an increase of paper surface roughness and a reduction of gloss, especially at low coating weight [11]. This is the reason for ink mottling increase, especially in the case of higher surface free energy (SFE) of coated paper [9].

The aim of the present work was to evaluate the influence of paper surface energy and fountain solution on mottling of printed surface at multicolor offset printing.

EXPERIMENTAL

Materials and methods

A series of commercial woodfree papers for multicolor offset printing was tested: two uncoated papers No. 35 and No. 58 (basis weight 120 g/m²); four glossy coated papers Nos. 38, 39, 55, and 57; and two semimatte coated papers No. 54 and No. 56 (basis weight 135 g/m²). The papers were from different European manufacturers. The range of paper characteristics is as follows:

- Surface roughness 0.89–5.89 µm (Parker Print Surf [PPS] method)
- SFE 29.8–40.4 mJ/m² (Owens, Wendt, Rabel, and Kaelble [OWRK] method; sessile drop, optical tensiometer OCA35, Dataphysics Instruments GmbH, Filderstadt, Germany)
- Mottling 5.7–18.3 (digital microscope DPM100, FIBRO System AB; Stockholm, Sweden)
- Formation index LT 20–25 for coated papers and LT 64–67 for uncoated papers (LAB 2D device, Techpap; Grenoble, France)
- Total area of pores and latex on coating surface OVS_{SEM} 7.8%–24.4 % (scanning electron microscope [SEM] image analysis of coating) [10,12]
- Mean pore size of uncoated papers D_{50} 1.6–2.0 µm (permeability method using ADP-2 pore size distribution analyzer, developed by the Pulp and Paper Research Institute; Bratislava, Slovak Republic).

Topography of paper surface

In general, topographic mapping requires scanning of the surface by a fine mechanism. There are many different types of sensors such as diamond engraving tools and various optical sensors, confocal and atomic force microscopes. Several instruments (Parker Print Surf [PPS] and Bekk, Bendtsen, and Sheffield methods) are suitable for surface roughness measurement by air permeability. The PPS permeability method (ISO 8791-4 "Paper and board—determination of roughness/smoothness [air leak methods]—part 4: print-surf method") is most commonly used to determine roughness, especially of smoother printing papers such as supercalendered and coated papers. PPS permeability and a photoclinometric method were used for the evaluation of paper surface roughness. Photoclinometry in the visible range of electromagnetic radiation [13,14] is a promising method that may be used for on-line measurement of paper roughness. It describes the process of transformation of a 2D surface image into a map of various height levels. Incident light creates shadows (different gray levels). Paper is an anisotropic material; therefore, it is necessary to obtain surface images from at least two directions: machine direction (MD) and cross direction (CD). The paper surface was scanned using charge-coupled device (CCD) Nikon Coolpix E4500 camera (Nikon; Tokyo, Japan) by inclined illumination at 10° from MD and CD.

Optical variability of surface OVS_{CLINO} was calculated from image analysis using the program ImageJ. It indicates a surface roughness in a similar manner to the roughness parameter Rq (average surface root means squared roughness), described in ISO 4287:1997 "Geometrical product specifications (GPS)—surface texture: profile method—terms, definitions and surface texture parameters."

Surface free energy

Initial and dynamic contact angle (CA), surface tension (γ) of liquids, as well as surface free energy (SFE) of paper were measured using the OCA 35 optical tensiometer. Contact angle was measured by sessile drop method. Wetting time was recorded by a CCD camera at the sequence 20 frames/s from the first contact of the liquid drop with the paper surface (0.05 s) through 5 s. Contact angle was calculated as the average of 10 parallel measurements. Several testing liquids (deionized water, low-viscous silicon oil, 16% aqueous solution of isopropyl alcohol [IPA], diiodomethane [DIM]) were used for CA measurements. Three testing liquids (DIM, ethylene glycol, thiodiglycol) with different surface tensions were used to determine SFE of paper. SFE, as well as its dispersive and polar components, was calculated by the OWRK method using values of initial CA. Pendant drop method was used to determine surface tension of the liquids.

Calculation of corrected CA and corrected SFE

Surface chemistry plays a key role in the control of absorption and adhesion phenomena at solid-liquid interfaces. Besides surface chemistry, topography and the chemical unevenness of surfaces are taken into account. Correction for the surface roughness [15] was calculated using the formula in Eq. (1):

$$r = 1 + \frac{S_{dr}}{100} \quad (1)$$

where S_{dr} is the roughness parameter that gives the real paper surface area with respect to the projected area as a percent increment; hence, S_{dr} = 0% refers to an ideally flat surface. Correction of roughness is always ≥ 1, whereby S_{dr} is calculated as 10 x PPS roughness. According to Wenzel's roughness equation, the relation between measured contact angle, CA_m, and Young contact angle, CA_Y, may be described as in Eq. (2):

$$\cos CA_m = r \cos CA_Y \quad (2)$$

From CA_Y of three testing liquids, corrected surface free energy, SFE_{CORR}, was calculated.

Dynamics of liquid absorption

Ultrasound intensity change was measured by the PDA C.02 ultrasound analyzer (Emtec; Radnor, PA, USA) within a period of 34 ms–30 s from the contact of coated paper surface with liquids. Testing liquids (surface tension γ, dynamic viscosity η at temperature 23 °C) were deionized water (72.8 mN/m, 0.9 mPa.s), 16% aqueous solution of IPA (44.2 mN/m, 1.1 mPa.s), silicon oil (19.9 mN/m, 15 mPa.s), and castor oil (35.0 mN/m, viscosity 800 mPa.s).



1. Printing test sheet with test elements.

Commercial printing

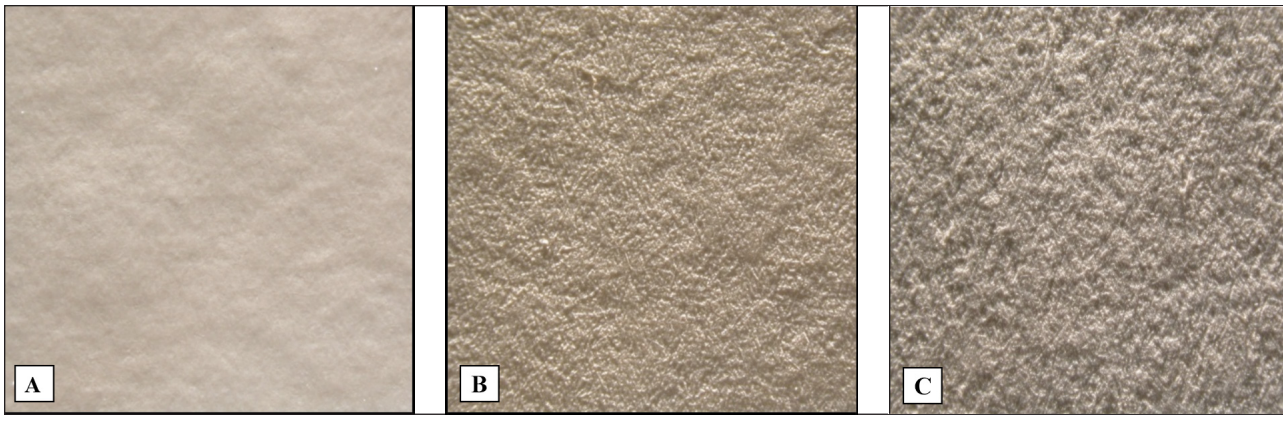
The printing press was a Heidelberg Speedmaster CD 74-6 (Heidelberger Druckmaschinen; Heidelberg, Germany), with full-automatic regulation of optical density according to preset criteria and printing conditions (ISO 12647-2 "Graphic technology— process control for the production of half-tone color separations, proof and production prints—part 2: offset lithographic processes"). Coated papers were printed with process inks having black (K) 1.8, cyan (C) 1.7, magenta (M) 1.7, and yellow (Y) 1.5 optical density and uncoated papers with inks having K 1.3, C 1.2, M 1.1, and Y 1.2 optical density.

The printing form parameters were an Agfa Azura 0.3-mm nonprocess negative printing plate (Agfa; Mortsel, Belgium), raster image processor (RIP) resolution of computer-to-plate (CTP) was 2400 DPI, screen ruling 175 LPI, round printing dot, and swingout of raster networks CMYK were 15°, 75°, 0°, 45°.The inks used were RAPIDA inks (Michael Huber Munchen; Kirchheim, Germany) for sheet offset; the order of inks was KCMY. The fountain solution was 3% IPA (Donauchem; Bratislava, Slovakia), 3% Saphira Fount 210 AR (Heidelberger Druckmaschinen; Heidelberg, Germany), with surface tension of 44.3 mN/m and temperature at 9°C.

The paper sheet size was 35 x 50 cm and the printing rate was 9000 sheets/h. Papers were printed sequentially on the top side at first. For print mottling evaluation were chosen 7-9 samples after 3000 prints. Subsequently, papers were printed in the same sequence on the back side. Printing machine data such as optical density of tone value increase and dot slur were monitored during printing. The printing test sheet with test elements is presented in **Fig. 1**.

Mottling

Mottling is evaluated by image analysis using different hardware and software solutions. Evaluation of original image as well as calculation and evaluation of spectral image prepared by fast Fourier transformation are well established [16–19]. Mottling was measured on the colored surface full printed by CMYK inks at the 3000th printed sheet. The conditions of mottling measurement were in conformity with ISO/IEC 13660:1997(E) "Information technology—office equipment—measurement of image quality attributes for hard copy output—binary monochrome text and graphic images standard," where mottling is expressed as periodic fluctuations of density at a spatial frequency less than 0.4 cycles/mm (or at a wavelength more than 2.5 mm) in all directions. Mottling measurement deals with dividing the original monochrome image into smaller cells at least 1.61 mm^2 in size and smallest dimension at least 1.27 mm. The measurement of mottling σ_i



2. Surface microtopography of (A) glossy coated, (B) semimatte coated, and (C) uncoated paper. (Photoclinometric method at 10° inclined illumination of surface in machine direction on top side of paper.)

across the region of interest of at least 161 mm² (i.e., 100 cells) was calculated as the standard deviation of the m_i, where m_i is the average of density measurements within cell i and n is total number of cells. The algorithm is described as Eq. (3):

$$\sigma_i = \sqrt{\sum_i \frac{m_i^2}{n}} \qquad (3)$$

Mottling evaluation was performed by measurement of the static image [8] prepared by the digital microscope DPM100. For the purpose of preserving text fluency in the following section, a simplified nomenclature for mottling was applied, using the combination of "mottling" and "color" of printed area with process inks, such as mottling K, mottling C, and so forth.

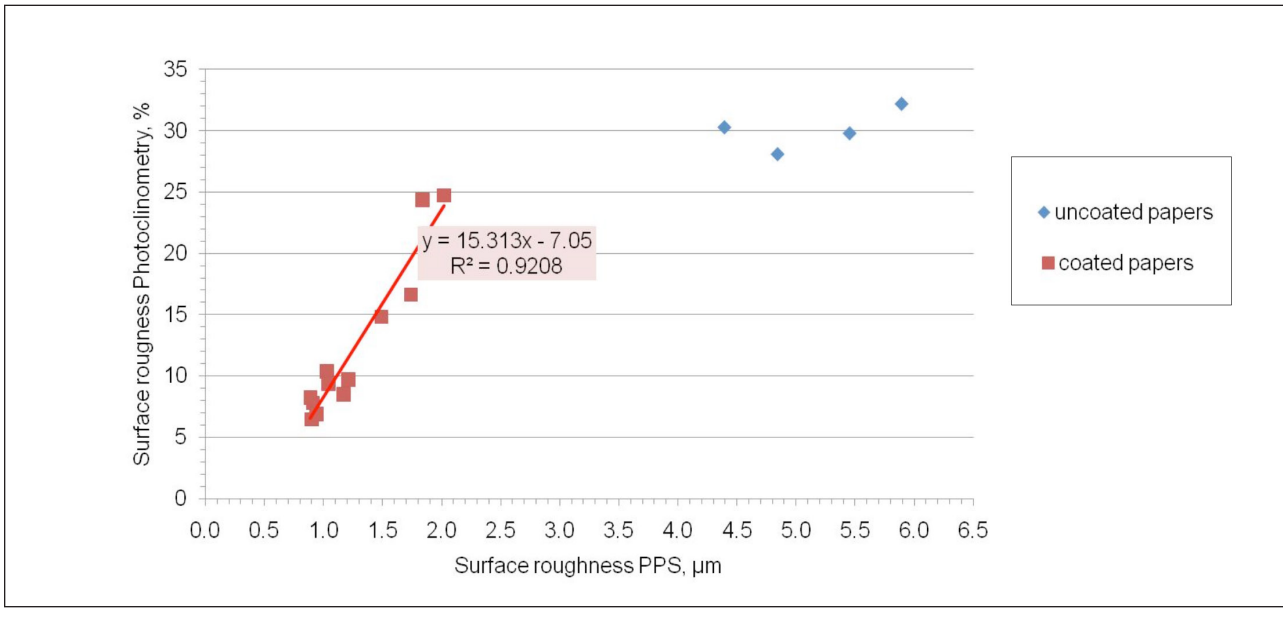
RESULTS AND DISCUSSION

Surface roughness

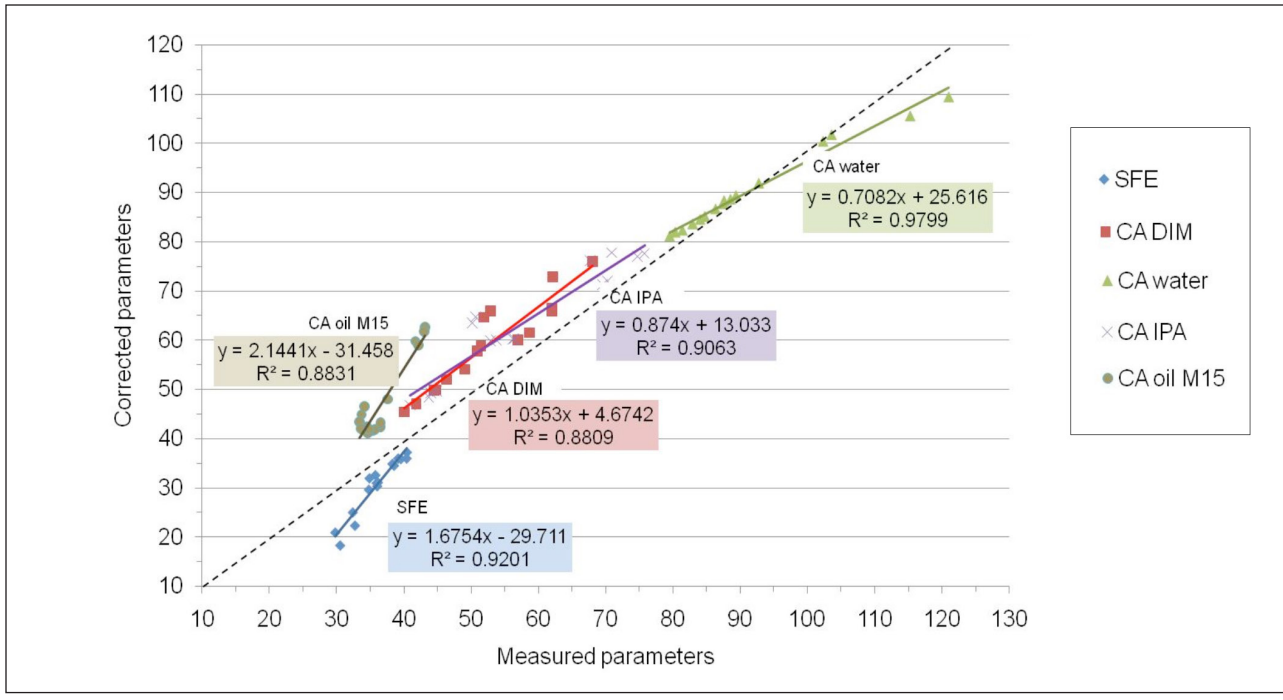
Surface roughness OVS_{CLINO} (mean value of surface optical variability) of the analyzed series of papers was within the range 7.8%–28.1%. This corresponds to PPS surface roughness of 0.89–5.89 µm. Microtopography of (A) glossy coated, (B) semimatte coated, and (C) uncoated paper is presented in **Fig. 2**.

Each paper has a unique structure in terms of surface roughness, porosity and surface free energy which is the result of manufacturing technology. **Fig. 3** shows the relation between both methods of surface roughness evaluation of coated and uncoated papers. The strength of relation of both methods expressed by coefficient of determination was very high in the case of coated papers (R^2 0.92).

Figure 4 shows the relation between the measured and



3. Relationship between optical method and Parker Print Surf (PPS) permeability method of microtopographic evaluation of paper surface (red dots = coated papers, blue dots = uncoated papers).



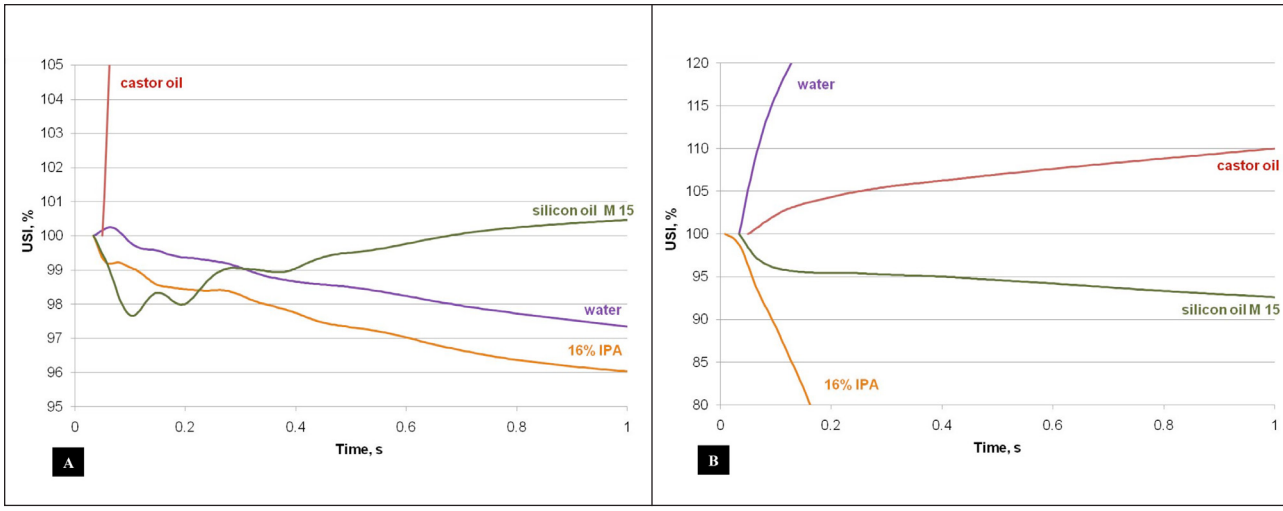
4. Relation between measured and corrected values of surface free energy (SFE) and contact angles (CA) of wetting with liquids of different surface tension. (Deionized water, 16% aqueous solution of isopropyl alcohol [IPA], diiodomethane [DIM], and silicon oil M15; series of coated and uncoated offset papers.)

CA_Y for liquids with different surface tension (deionized water, 16% aqueous solution of IPA, DIM, and silicon oil M15) and the relation between SFE before and SFE_{CORR} after correction (Wenzel) on an ideally flat surface. The curves show papers with higher roughness further from the axis (dotted-and-dashed line) of an ideally flat surface. In the case of wetting of the surface with water, the CA values of hydrophobic rough surface ($CA_m \geq 90°$) of uncoated papers were higher than it would be valid for an ideally flat surface. In the case of hydrophilic surfaces of coated papers ($CA_m \leq 90°$), CA for water are always lower than in case of any other liquid with a lower surface tension (16% aqueous solution of IPA, DIM, and silicon oil M15). Thus, the data show that surface roughness will enhance the wetting of hydrophilic surfaces and reduce the wetting of hydrophobic surfaces.

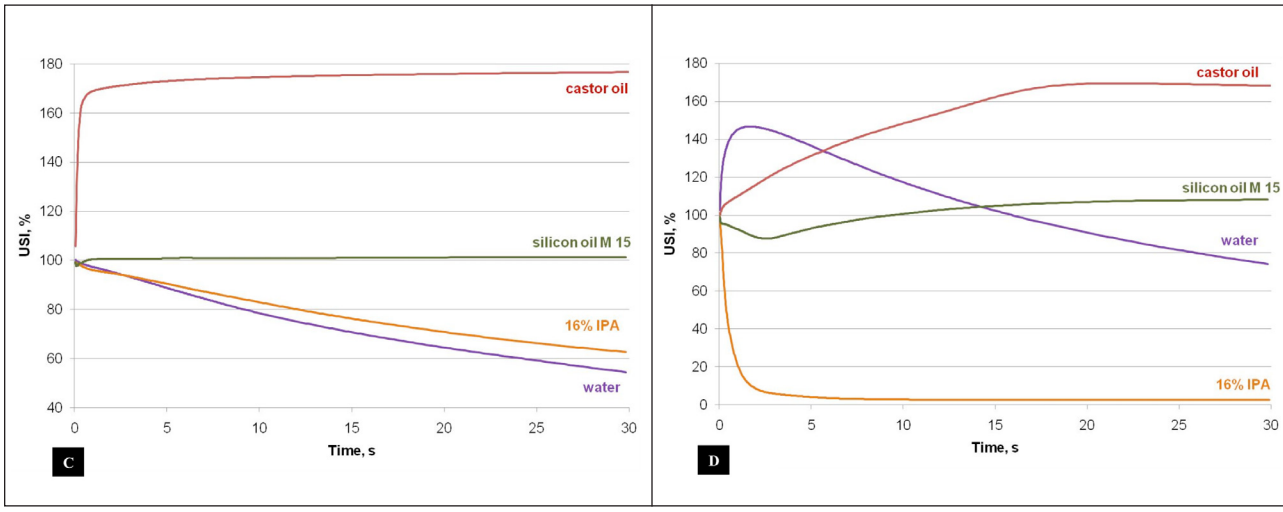
At the contact of liquid with paper surface, imbibition (a dynamic process of liquid absorption by a substance) occurs, involving phenomena such as wetting, penetration, diffusion, and swelling. Ultrasound measurement of this dynamic process enabled an assessment of the difference in the quality of coated and uncoated papers [10,20]. In the study of interactions between offset papers and liquids [20],the following properties were evaluated: surface roughness by ultrasound signal intensity (USI) in 70 ms (USI_{70}) after first contact of paper with water and fine-pores content (t_{95}) by the time required for reduction of USI from 100% to 95% at contact with paper with 16% water solution of IPA. Both acquired parameters (USI_{70} and t_{95}) showed correlation (R 0.93–0.95) with PPS roughness and print density. Monitoring of USI dynamics at contact of uncoated paper and liquids with various surface tension and viscosity [10] and its correlation with the area of surface pores and surface latex, as well as with rate of printing ink setoff, confirmed correctness of evaluation and interpretation of coating SEM image.

Figure 5 shows the intensity of transmitted USI, which changes due to the effects of testing liquids on the surface of coated paper with SFE 35.7 mJ/m² (image A) and uncoated papers with SFE 32.7 mJ/m² (image B) within a period of 34 ms up to 1 s. Different dynamics of surface wetting and penetration is a result of liquids properties, sizing, surface roughness, fine-pores content, and presence of components capable of swelling in the applied liquid.

In the case of coated paper, the surface was wetted with water in a time below 100 ms (maximum on blue curve image A in Fig. 5). Aqueous solution of IPA and low-viscous silicon oil M15 wetted the surface and penetrated into the coating immediately. After 100 ms the course of USI silicon oil M15 signal (green curve of image A) is different from the course of USI water signal and aqueous solution of IPA. During the course of fast penetration, oil does not cause swelling of fibers in paper as is the case with water and water solutions. High-viscous castor oil cannot penetrate into coated paper in a short time; therefore, the USI signal increased steeply (red curve of image A). After the steep increase of the USI signal in the 1st second, the signal slowly increased even in the 30th second (image C in **Fig. 6**). After a few seconds, the penetration USI signal of silicon oil did not change further (image C in Fig. 6). Scanning electron microscope analysis of the coating surface and printing ink setoff rate showed that USI of high-



5. Intensity of transmitted ultrasound signal at the contact of top side of coated paper (image A) and uncoated paper (image B) with water (blue curve), 16% aqueous solution of IPA (yellow curve), silicon oil (green curve), and castor oil (red curve). (The properties of coating: SFE 35.7 mJ/m², PPS 0.91 µm, surface pores and latex area [OVS_{SEM}] 18.8%, size of surface pores less than 200 nm. The properties of uncoated surface: SFE 32.7 mJ/m², PPS 5.9 µm, mean pore size 2.0 µm. The ratio of surface tension and viscosity of test liquids: water 80.9 m/s, aqueous solution of IPA 40.2 m/s, silicon oil 1.33 m/s, and castor oil 0.04 m/s.)



6. The intensity of transmitted ultrasound signal at the contact of top side of coated paper (image C) and uncoated paper (image D) with water (blue curve), 16 % aqueous solution of IPA (yellow curve), silicon oil (green curve), and castor oil (red curve).

viscous castor oil in a period of 10–30 s correlates with total area of surface pores and surface latex in the coating. Analyses also showed that the USI signal of low-viscous silicon oil M15 correlates only with the area of coating surface pores.

In the case of uncoated paper (image B in Fig. 5), the aqueous solution of IPA and silicon oil M15 immediately penetrates and the porous paper is saturated in 2–3 s. The pores of uncoated paper are large, and the high-viscous castor oil penetrates comparatively quickly. Water is wetting the surface of uncoated paper in 2–3 s and only afterwards penetrates into paper (image D in Fig. 6).

Images C and D in Fig. 6 show the ultrasound intensity change in a time interval up to 30 s. Surface tension and dynamic viscosity of liquids at 23°C was in the range of γ 20.0–72.8 mN/m and η 0.9-800 mPa.s. Water and aqueous solution of IPA caused a decrease of the ultrasound signal that identifies liquid penetration. Decrease of the ultrasound signal is caused by displacement of air by liquid and formation of air bubbles with diameters of a few micrometers, on which scattering of the ultrasound signal occurs to an increased extent. By using water, it is possible to observe a striking maximum in the case of both papers (blue curve of image A in Fig. 5 and image D in Fig. 6). In the time of maximum achievement, wetting of surface is finished and penetration and swelling starts. The occurrence and time shift of the maximum identifies the time-limited partial hydrophobicity of surface, the so-called degree of sizing. This can be used to understand the ink transfer and water sensitivity mottle (WIM) in a single

printing unit, as will be presented later.

When using a low-viscous silicon oil with a surface tension and viscosity ratio of 1.33 m/s, a short-time decrease of ultrasound signal up to 100 ms was observed in the case of coated paper (green curve of image A in Fig. 5). Later on, the ultrasound signal increases, reaching the initial value (100%) at 700 ms followed by a slight increase up to 30 s of observation (green curve of image A in Fig. 5 and image C in Fig. 6). However, in the case of high-viscous castor oil with a ratio of surface tension and viscosity of 0.04 m/s, the ultrasound signal does not decrease but steeply increases within a time to 200 ms; in the case of coated paper it further mildly increases until the 30th s of observation (red curve of image C in Fig. 6).

In real conditions on a printing press, various combinations of ink-water occur at the point of printing of ink on paper. The application of water in subsequent printing units causes ink equalization and decreases mottling effect. Deposition of a second color (on a once-wetted paper surface) and its reverse cleavage results in a reduction of mottling effect. In conjunction with double equalization by water in the third and fourth printing units, the best printing result may be expected. When the water amount on paper is increased due to wetting in the second printing unit, an increase of mottling effect of ink applied in the third printing unit may be expected. These published findings [2,3] were applied to set up the order of inks and to evaluate full-scale printing in the Heidelberg Speedmaster CD-74-6 printing press. Black ink (K) was applied as the first one in the sequence; it was printed on a dried surface and in the next three printing units, fountain solution replaced the ink. This printing technique is labeled as KWWW (black-water-water-water).

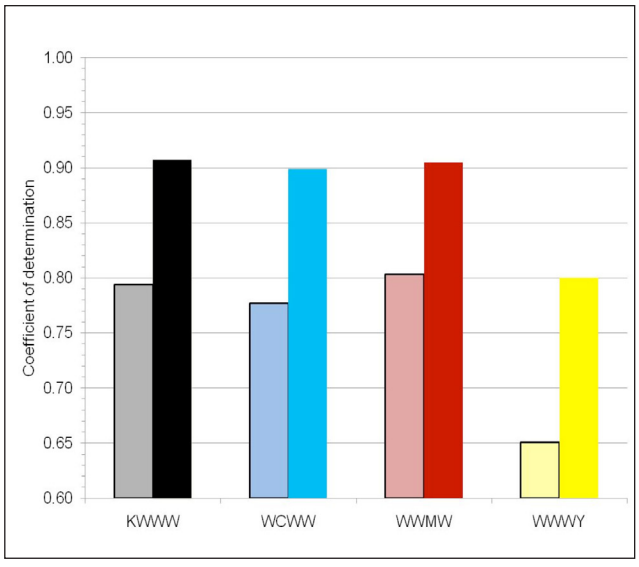
Cyan ink (C) was applied as the second one, on a paper surface once wetted by fountain solution from the first printing unit. Fountain solution was applied on surface printed by ink C in the next two printing units. This process is marked as WCWW (water-cyan-water-water). Magenta ink (M) was applied on twice-wetted paper surface and fountain solution was applied on the surface printed by M ink in the last printing unit. This process is marked as WWMW (water-water-magenta-water). Yellow ink (Y) was applied as the last one in the sequence on a thrice-wetted paper surface. This process is marked as WWWY (water-water-water-yellow).

In **Table I**, the order of papers is listed according to mottling in the first to fourth printing units of the Heidelberg Speedmaster CD-74-6 press. The values of mottling are shown by pairs of numbers (for top/back side of paper). It is interesting that the semimatte coated paper No. 56 reached about a two-times higher mottling in comparison with rougher uncoated papers No. 35 and No. 58. The fountain solution significantly compensated the negative influence of uncoated papers surface roughness on mottling. Back-trap mottling of uncoated papers without application of fountain solution in laboratory printing by Amsterdam 1 Printability Tester (IGT Testing Systems; Amsterdam, The Netherlands) was as high as 16–19. Back-trap mottling of semimatte paper No. 56 in laboratory printing was 7.7–7.8. Application of fountain solution in the printing press on printing paper No. 56 caused an increase of mottling in combinations KWWW, WWMW, and WCWW to a level of 10.5–15.3, which shifted this paper to the last place in the quality order in Table I.

A comparison of permeability and optical method of surface roughness measurement of coated papers with regard to mottling K, C, M, and Y is presented in **Fig. 7**. The influence of surface roughness PPS of coated papers at printing by black ink on mottling is very powerful (R^2_K 0.80). Mottling of printed surface in other printing units showed a similarly strong dependence on PPS roughness of coated papers (R^2_C 0.78, R^2_M 0.80, R^2_Y 0.65). The photoclinometric method of surface

Combination	Order	1	2	3	4	5	6	7	8
KWWW Print Unit 1	Mottling	4.5/4.5	5.1/4.9	5.8/5.7	6.5/7.0	6.8/6.8	6.7/7.1	7.4/7.0	15.3/14.9
	Paper No.	39	38	57	35	58	55	54	56
WCWW Print Unit 2	Mottling	5.1/4.8	5.4/5.3	5.6/5.7	5.8/6.0	6.4/6.1	7.3/7.6	7.5/7.5	10.5/10.3
	Paper No.	38	39	57	55	54	35	58	56
WWMW Print Unit 3	Mottling	5.6/5.1	5.6/5.4	5.5/5.8	5.8/5.8	7.0/6.4	7.5/7.2	8.0/7.1	13.6/13.5
	Paper No.	39	38	35	58	57	55	54	56
WWWY Print Unit 4	Mottling	1.9/2.0	2.1/2.2	2.3/2.3	2.3/2.3	2.5/2.2	2.7/2.5	2.8/2.8	5.6/5.7
	Paper No.	39	38	57	35	54	58	55	56

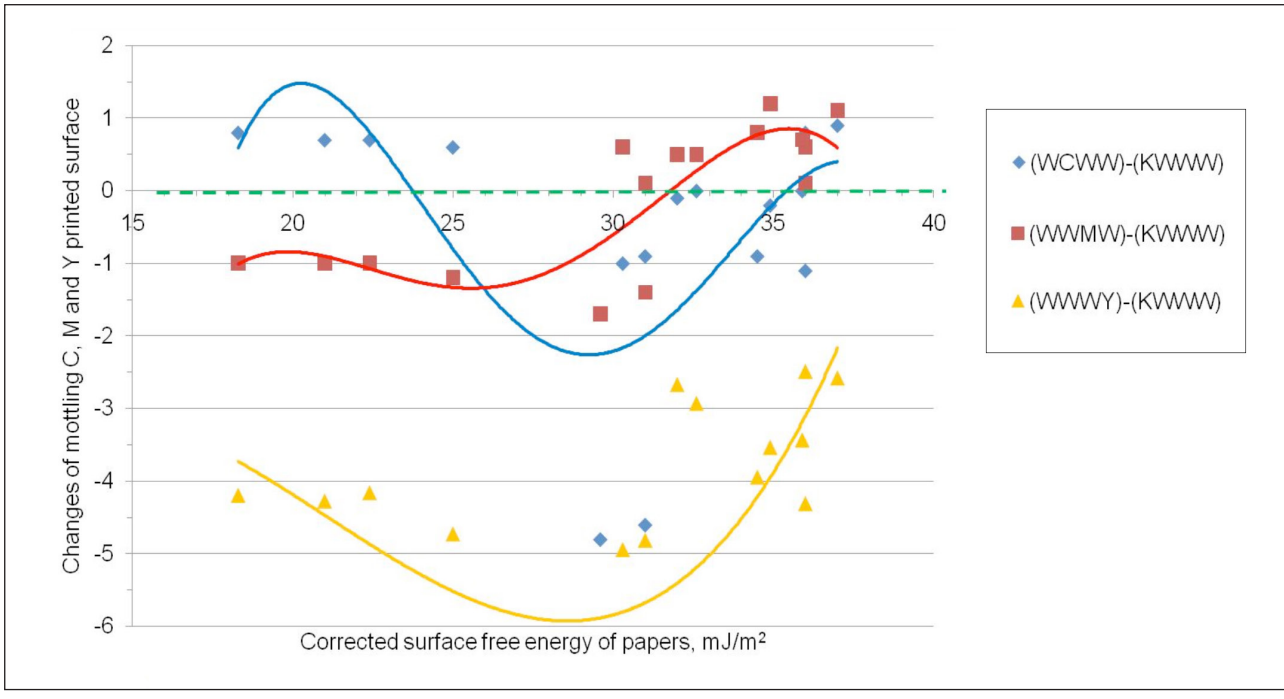
I. Order of papers in relation to mottling evaluated on printed surfaces K, C, M, and Y.



7. Strength of relationship between mottling K, C, M, Y and coated paper topography. Light-colored framed columns indicate the PPS permeability method and darker columns indicate the photoclinometric method. (Printing on a Heidelberg Speedmaster CD-74-6 press.)

roughness evaluation (OVS_{CLINO}) enables a significant increase in the strength of the relationship to mottling (R^2_{CMYK} 0.80–0.91) in comparison with the permeability method (PPS).

Within the range of SFE of evaluated papers, (SFE 29.8–40.4 mJ/m²), SFE was found to have no influence on mottling K (mottling of surface printed with black ink in the first printing unit). Mottling C, M, and Y obtained by printing process in the second to fourth printing units in the combinations WCWW, WWMW, and WWWY showed changes depending on paper surface energy in comparison with the printed surface K. In **Fig. 8**, the change of mottling in the second (C) to the fourth printing unit compared to mottling in the first printing unit is presented in relation to paper surface energy. Values of SFE of paper corrected in respect of an ideally flat surface are shown on the x axis. In the range of hydrophobic surface SFE_{CORR} 18-25 mJ/m² (uncoated papers), mottling C is higher by 0.6–0.8 compared to mottling K. The paper cannot in a short time absorb water and therefore C ink transfer is abnormal. The curve of mottling C has a clear minimum at SFE_{CORR} from 27 mJ/m² to 31 mJ/m², and mottling even at SFE_{CORR} 35 mJ/m² is still lower than mottling K. In this case, paper allows water to penetrate and C ink transfer is normal. In the third printing unit into which paper enters already twice wetted, mottling M is lower by 1.0–1.2 compared to mottling K in the range of SFE_{CORR} from 18 mJ/m² to 30 mJ/m². Paper allows water to penetrate in a twice-longer time than ink C and ink transfer is normal. With the next increase of surface energy (by increasing paper surface hydrophility), when higher reception of fountain solution occurs, mottling M is higher by 0.5–1.2 in comparison with mottling K. The change of mottling Y in relation to SFE_{CORR} is very similar to the course of mottling M. Increases of C, M, and Y mottling of paper with SFE_{CORR} higher than 35 mJ/m² can be attributed to swelling of pulp fibers by wetting solution, which increases surface roughness of paper.



7. Strength of relationship between mottling K, C, M, Y and coated paper topography. Light-colored framed columns indicate the PPS permeability method and darker columns indicate the photoclinometric method. (Printing on a Heidelberg Speedmaster CD-74-6 press.)

Mottling evaluation of multicolor offset printing showed how mottling in the second, third, and fourth printing units is influenced by paper surface roughness and surface energy, as well as by the amount of fountain solution absorbed by the paper surface.

CONCLUSIONS

To understand the origin of phenomena such as print mottling and printing ink setoff in the multicolor printing process, it is certainly necessary to analyze the following eight properties: (1) surface tension of liquid, (2) dynamic viscosity of liquid, (3) ability of liquid to swell coating and base paper components (latex binder and pulp fibers), (4) paper surface roughness, (5) paper SFE, (6) fine pores content in paper, (7) area of surface pores in coating, and (8) area of surface latex binder in coating.

For hydrophobic surface uncoated papers with SFE_{CORR} 18–25 mJ/m², mottling C was higher by 0.6–0.8 compared to mottling K. Paper cannot in a short time accept water and therefore C ink transfer was abnormal. Mottling C has a clear minimum at SFE_{CORR} from 27 mJ/m² to 31 mJ/m², and mottling even at SFE_{CORR} 35 mJ/m² was still lower than mottling K. In this case, paper allows water to penetrate and C ink transfer was normal.

In the third printing unit into which paper enters already twice wetted, mottling M was lower by 1–1.2 compared to mottling K in the range of SFE_{CORR} from 18 mJ/m² to 30 mJ/m². Paper allows water to penetrate (in twice-longer time than with ink C) and, therefore, ink transfer was normal. With the next increase of surface energy, when higher reception of fountain solution occurs, mottling M was higher by 0.5–1.2 in comparison with mottling K.

The change of mottling Y in relation to SFE_{CORR} was very similar to the course of mottling M. Increase of mottling C, M, and Y of paper with SFE_{CORR} higher than 35 mJ/m² can be attributed to pulp fibers swelling, which increases surface roughness of coated paper.

Application of fountain solution significantly influenced mottling of both uncoated (rough) papers No. 35 and No. 58 and a coated semimatte paper No. 56 with highest roughness. In laboratory printing by the Amsterdam 1 Printability Tester, high mottling was expected in the case of uncoated papers (BTM standard C ink 16–19), which would copy surface roughness. Influence of fountain solution in printing-press mottling was reduced in each printing unit (in combination WCWW to 7.3–7.6) and to the highest extent in combination WWMW to 5.5–5.8 This finding is logical with regard to low SFE of uncoated paper and slower absorption of wetting solution. In the case of higher-roughness semimatte paper, application of fountain solution had negative influence. For paper No. 56, BTM measured in the laboratory was 7.7–7.8; mottling in commercial printing increased in every printing unit (in combinations KWWW, WWMW, and WCWW to 10.5–15.3).

ABOUT THE AUTHORS

Our long-term work is focused on systematic research of barrier and surface properties of paper and on application of various raw materials required for paper manufacture. This work is aimed at a better understanding of combined influence of surface free energy, surface roughness, and fountain solution on print mottling occurring on uncoated and coated papers in the multicolor offset printing process.

This new study is continuation of our previous works published in *Nord. Pulp Paper Res. J.* 28(2): 274(2013) and 28(3): 443(2013) in which we studied influence of surface structure (roughness and porosity) of coating on ink setting time and on mottling.

The most difficult aspect of this research was the generation of a complex view of particular parameters that effect the printing processes and print quality. We discovered that the dynamics of wetting, penetration and diffusion depends on a combination of liquids and solid porous materials properties such as surface tension of liquids, dynamic viscosity of liquids, ability of liquids to swell coating and base paper components, surface roughness, surface free energy, area of surface pores, and area of surface latex binder in coating. Mottling can be minimized by the choice of optimal paper from the point of view of surface free energy and surface roughness. There is a relatively small range of surface free energy for minimization of mottling.



Gigac



Kasajová



Stankovská

The results of this work can be used by paper manufacturers and converters of paper, as well as by printers, to achieve optimum print quality. The next step in our research has already started. We are continuing the study focused on liquids imbibition dynamics on the surfaces of micro-porous media such as ink-jet paper and paper-based packaging.

Gigac is senior scientist and head of the paper division, Kasajová is a researcher, and Stankovská is a scientist at the Pulp and Paper Research Institute, Bratislava, Slovak Republic. Email Gigac at gigac@vupc.sk.

It is assumed that this can be caused by a combination of slower ink setting rate, slower SFE, and higher surface roughness. **TJ**

ACKNOWLEDGEMENTS

The results were achieved in the framework of the basic research project "Interactions of liquids with paper surface" of the applied research project "Conversion of technology of fluting production in Smurfit Kappa Štúrovo" and of the technical feasibility study "Increasing the utility of the adhesives and the adhesive mixtures for wood industry and pulp and paper industry with incorporation of selected nanoparticles." This work was supported by the Ministry of Education, Science, Research and Sport of the Slovak Republic under law No. 185/2009 regarding stimulus of R&D. Many thanks go to printing shop SINEAL, s. r. o., for realization of the full-scale printing test.

LITERATURE CITED

1. Kaplanová, M., *Moderní polygrafie*, Svaz polygrafických podnikatelů, Prague, Czech Republic, 2009, p. 298.
2. Klein, R., Miletic, M., Meder, G., et al., *Wochenbl. Papierfabr.* 139(5): 324 (2011).
3. Klein, R., Miletic, M., Meder, G., et al., *Wochenbl. Papierfabr.* 139(6): 464 (2011).
4. Whalen-Shaw, M. and Eby, T., *Tappi J.* 74(12): 188(1991).
5. Plowman-Sandreuter, N., *Tappi J.* 77(7): 173(1994).
6. Ness C., Praast H., Renner K., et al., *Das Papier* 46(11): 641(1992).
7. Enomae, T. and Onabe, F., *Sen´i Gakkaishi* 53(3): 86(1997).
8. Kasajová, M. and Gigac, J., *Nord. Pulp Pap. Res. J.* (28)3: 443(2013).
9. Gigac, J., Fišerová, M., Kasajová, M., et al., "Mikrotopografia, pórovitost', povrchová energia a potlačiteľnost' papiera (Microtopography, porosity, surface energy and printability of paper)," *AKZO Nobel Meet.*, Karlštejn, Czech Republic, May 2012.
10. Gigac, J., Kasajová, M., Maholányiová, M., et al., *Nord. Pulp Pap. Res. J.* 28(2): 274(2013).
11. Hallamaa, T., Heikkurinen, A., Forström, U., *TAPPI Int. Mech. Pulping Conf., Proc.*, TAPPI PRESS, Atlanta, GA, USA, 1999, p. 57.
12. Chinga, G. and Helle, T., *Nord. Pulp Pap. Res. J.* 14(3): 307(2002).
13. Korokhin, V.V., Velikodsky, Y.V., Shkuratov, Y.G., et al., *Planet. Space Sci.* 58(10): 1298 (2010).
14. Kiviranta, A. and Paulapuro, H., *Tappi J.* 75(4): 172(1992).
15. Tåg, C.M., Juuti, M., Peiponen, K.-E., et al., *Coll. Surf. A* 317(1-3): 659(2008).
16. Fahlcrantz, C-M., Johansson, P.-A., and Aslund, P., *J. Imaging Sci. Technol.* 47(1): 54(2003).
17. Christoffersson, J., "Evaluation of systematic and colour print mottle," Master's thesis, Linköping Institute of Technology, Linköping University, Linköping, Sweden, 2004.
18. Sadovnikov, A., Salmela, P., Lensu, L., et al., *14th Scandinavian Conf. Image Analy., Proc.*, Springer-Verlag Berlin-Heidelberg, 2005, p. 409.
19. Keller, G., *PTSNews* 2:16(2009). Available [Online] http://www.ptspaper.com/fileadmin/PTS/Dokumente/Unternehmen/PTS_News/News_2009_02_engl.pdf.
20. Gigac, J., Stankovská, M., and Kasajová, M., *Wood Res.* 56(3): 363(2011).

IBBC 2014

International Bioenergy & Bioproducts Conference

September 17-19, 2014
Tacoma, Washington USA

No matter how you calculate it,
IBBC=BioIQ^n

Get a Fresh Look at Biomass Utilization

at the only industry event in North America dedicated to advancing biorefineries in the forest products industry.

Biomass Supply and Demand
Assessments, Sources, and Physical Properties

Biomass Harvesting and Preparation
Equipment, Processing, Pretreatments, and Characterization

Advances in Conversion Pathways
Biochemical and Thermochemical Technologies

Bioproducts
Fuels, Chemicals, and Energy

Economic Assessments
Mill Experiences, Collaborations, and Economic Assessments

Co-Located with:
PEERS
SEPTEMBER 14-17, 2014
Tacoma, Washington

Program • Speakers • Updates
tappi.org/14ibbc